Journal Pre-proofs

Design, synthesis, and biological evaluation of tetrahydroquinolin derivatives as potent inhibitors of CBP bromodomain

Yu Chen, Xiaoyang Bi, Fengcai Zhang, Zhongya Sun, Pan Xu, Hao Jiang, Wenchao Lu, Tian Lu, Hong Ding, Naixia Zhang, Hualiang Jiang, Kaixian Chen, Bing Zhou, Cheng Luo

Please cite this article as: Y. Chen, X. Bi, F. Zhang, Z. Sun, P. Xu, H. Jiang, W. Lu, T. Lu, H. Ding, N. Zhang, H. Jiang, K. Chen, B. Zhou, C. Luo, Design, synthesis, and biological evaluation of tetrahydroquinolin derivatives as potent inhibitors of CBP bromodomain, *Bioorganic Chemistry* (2020), doi: https://doi.org/10.1016/j.bioorg.2020.103991

This is a PDF file of an article that has undergone enhancements after acceptance, such as the addition of a cover page and metadata, and formatting for readability, but it is not yet the definitive version of record. This version will undergo additional copyediting, typesetting and review before it is published in its final form, but we are providing this version to give early visibility of the article. Please note that, during the production process, errors may be discovered which could affect the content, and all legal disclaimers that apply to the journal pertain.
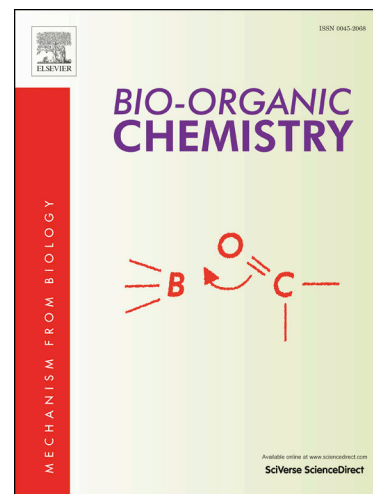
Design, synthesis, and biological evaluation of tetrahydroquinolin derivatives as potent inhibitors of CBP bromodomain

Yu Chen[a,b,#], Xiaoyang Bi[b,c#], Fengcai Zhang[d], Zhongya Sun[a,e], Pan Xu[a,b], Hao Jiang[a,b], Wenchao Lu[f],Tian Lu[a,g], Hong Ding[a,*], Naixia Zhang[h], Hualiang Jiang[a,b], Kaixian Chen[a,b,i], Bing Zhou [b,c,*], Cheng Luo [a,b,i,*]

[a] Drug Discovery and Design Center, State Key Laboratory of Drug Research, CAS Key Laboratory of Receptor Research, Shanghai Institute of Materia Medica, Chinese Academy of Sciences, 555 Zuchongzhi Road, Shanghai 201203, China

[b] University of Chinese Academy of Sciences, 19 Yuquan Road, Beijing 100049, China

[c] Department of Medicinal Chemistry, Shanghai Institute of Materia Medica, Chinese Academy of Sciences, 555 Zuchongzhi Road, Shanghai 201203, China

[d] School of Pharmacy, Nanchang University, Nanchang, 330006, China

[e] School of Life and Technology, Harbin Institute of Technology, Harbin, 150001, China

[f] Department of Cancer Biology, Dana-Farber Cancer Institute, Boston, MA, 02215, USA

[g]Jiangsu Key Laboratory for High Technology Research of TCM Formulae, Nanjing University of Chinese Medicine, 138 Xianlin Road, Nanjing 210023, China

[h] Department of Analytical Chemistry, Shanghai Institute of Materia Medica, Chinese Academy of Sciences, 555 Zuchongzhi Road, Shanghai 201203, China

[i] Open Studio for Druggability Research of Marine Natural Products, Pilot National Laboratory for Marine Science and Technology (Qingdao), 1 Wenhai Road, Aoshanwei, Jimo, Qingdao 266237, China

[#]These authors contributed equally.

*Corresponding authors

Hong Ding: hding@simm.ac.cn

Bing Zhou: zhoubing@simm.ac.cn.

Cheng Luo: cluo@simm.ac.cn

Abstract

CREB-binding protein (CBP) is a large multi-domain protein containing a HAT domain catalyzing transacetylation and a bromodomain responsible for acetylated lysine recognition. CBPs could act as transcription co-activators to regulate gene expression and have been shown to play a significant role in the development and progression of many cancers. Herein, through *in silico* screening two hit compounds with tetrahydroquinolin methyl carbamate scaffold were discovered, among which **DC-CPin7** showed an *in vitro* inhibitory activity with the TR-FRET IC_{50} value of 2.5 ± 0.3 μM. We obtained a high-resolution co-crystal structure of the CBP bromodomain in complex with **DC-CPin7** to guide following structure-based rational drug design, which yielded over ten **DC-CPin7** derivatives with much higher potency, among which **DC-CPin711** showed approximately 40-fold potency compared with hit compound **DC-CPin7** with an *in vitro* TR-FRET IC_{50} value of 63.3 ± 4.0 nM. Notably, **DC-CPin711** showed over 150-fold selectivity against BRD4 bromodomains. Moreover, **DC-CPin711** showed micromolar level of anti-leukemia proliferation through G1 phase cell cycle arrest and cell apoptosis. In summary, through a combination of computational and crystal-based structure optimization, **DC-CPin711** showed potent *in vitro* inhibitory activities to CBP bromodomain with a decent selectivity towards BRD4 bromodomains and good cellular activity to leukemia cells, which could further be applied to related biological and translational studies as well as serve as a lead compound for future development of potent and selective CBP bromodomain inhibitors.

1.Introduction

Adenovirus E1A-associated 300-kD protein (EP300, P300) and CREB-binding protein (CREBBP, CBP) are sequence and evolutionary conserved mammalian-specific histone acetyltransferases, and hence they are always been mentioned together[1-3]. CBP/P300 (hereinafter referred to as "CBP") is a large multi-domain protein [3]. In addition to its catalytic HAT domain, which weakens the association between positively charged histones and negatively charged DNA by acetylating the N-terminal histone tail, it also contains a bromodomain that recognizes and binds to the acetylated histones[4]. CBP bromodomain is an important member of the non-BET bromodomain family, which could participate in transcription regulating programs and regulate gene expression by functioning as transcription co-activators. Besides, CBP bromodomain has been proven to regulate MYC[5, 6], a transcription factor and oncogene widely overexpressed in varieties of cancers [7-10], shedding light on the potential therapeutic effects of CBP bromodomain inhibition on cancers like hematologic malignancies. An increasing amount of studies are devoted to the development of CBP bromodomain inhibitors in the light of good interplay between the development of BET chemical probes and biological studies of BET bromodomains. SGC-CBP30 was optimized from known BET inhibitor scaffolds 5- and 6-isoxazolylbenzimidazoles, which could potently bind to CBP with a TR-FRET IC_{50} of 21nM[11]. Steven Magnuson's group adopting a fragment-based screening or high throughput screening followed iterative chemical optimization has discovered highly potent CBP bromodomain inhibitors CP1-736[12], GNE-272[13]and GNE-781[14].A figure

summary of the structures and activities of selected CBP bromodomain inhibitors reported in the literature was included in the Supplementary Figure 1. All these inhibitors could provide high-quality chemical probes for further biological function of CBP bromodomain and promote the development of therapeutic agents of CBP-related malignancies.

Herein, through *in silico* screening we identified two CBP bromodomain hit compounds with micromolar level of inhibitory activities. Based on a co-crystal of **DC-CPin7** and CBP bromodomain we obtained, structure-based chemical optimization strategies were successfully used to attain **DC-CPin711**, a potent inhibitor with a 40-fold inhibitory activity against CBP bromodomain compared with hit compound **DC-CPin7**. Notably, **DC-CPin711** showed over 150-fold selectivity against BRD4 bromodomains. Moreover, **DC-CPin711** could significantly inhibit cell proliferation and decrease c-Myc level in a dose-dependent manner in MV4-11 leukemic cells. Further experiments validated its leukemic cell-killing activity through G1 phase cell cycle arrest and cell apoptosis. **DC-CPin711** represents a promising lead compound of CBP bromodomain for further optimization.

2.Results

2.1. Discovery and preliminary biological evaluation of hit compound DC-CPin6 and DC-CPin7

In silico screening as a powerful computational approach to identify hit compounds by predicting the affinity of large libraries of chemical structures binding to the desired drug target, can reduce the actual number of compounds needed to be screened. It has emerged as an important tool to improve hit compound discovery efficiency. This strategy has been

successfully applied in the discovery of inhibitors targeting varieties of proteins including GLUT5[15],GTPase[16] as well as CBP histone acetyltransferase domain[17, 18]. Previous literature has reported an *in silico* screening of 1413 fragments against CBP bromodomain to obtain two micromolar fragments with favorable ligand efficiency[19]. In this study, we utilized molecular docking-based *in silico* screening trying to identify novel inhibitors of CBP bromodomain from an in-house chemical database containing approximately 364,000 diverse and PAINS filtered compounds (Figure 1A). Standard Precision (SP) mode and flexible ligand sampling in Glide module was been adopted to conduct molecular docking-based *in silico* screening and score ligands in the chemical database. The top 1000 compounds were picked out to perform further cluster analysis and visual inspection to ensure the chemical diversity of candidate compounds to be purchased. The CBP bromodomain inhibitory activities of the 105 candidates selected were tested by homogeneous time resolved fluorescence assays. Among them, **DC-CPin6** and **DC-CPin7** showed moderate CBP bromodomain inhibitory activities, with the IC_{50} value of 10.5 ± 1.0 μM and 2.5 ± 0.3 μM respectively (Figure 1B and 1C). The *in vitro* activities of **DC-CPin6** and **DC-CPin7** were further investigated via ligand-based NMR spectroscopy and protein thermal shift assays. In the Carr-Purcell-Meiboom-Gill (CPMG) NMR experiment, the addition of CBP bromodomain led to a dose-dependent decrease of NMR signal in **DC-CPin6** and **DC-CPin7**, suggesting the direct binding between CBP bromodomain and the two hits (Figure 1D and 1E).

Then, in the protein thermal shift assays, **DC-CPin6** and **DC-CPin7** induced Tm shifts for 2.3℃ and 4.1℃ respectively (Figure 1F). The greater Tm shift induced by **DC-CP71** was in accordance with their IC_{50} values. Taken together, these biophysical data validated

DC-CPin6 and **DC-CPin7** could bind to CBP bromodomain directly. Moreover, **DC-CPin7**

showed a greater *in vitro* inhibitory activity, which served as the hit for our further
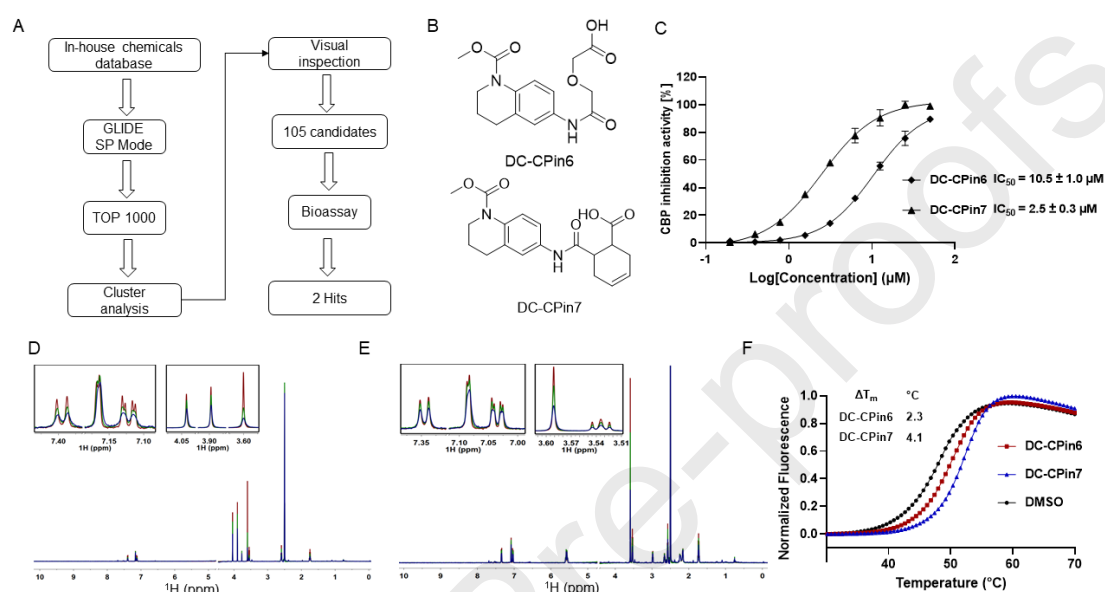
optimization.

Figure 1. The discovery of **DC-CPin6** and **DC-CPin7** as moderate CBP bromodomain inhibitor. (A) The flowchart of molecular docking-based *in silico* screening. (B) The chemical structure of **DC-CPin6** and **DC-CPin7**. (C)The *in vitro* activities of **DC-CPin6** and **DC-CPin7** measured by HTRF. (D-E) The CPMG NMR spectrum of **DC-CPin6** and **DC-CPin7** respectively. (F) The protein thermal shift assays of **DC-CPin6** and **DC-CPin7** on CBP bromodomain.

2.2 The binding mode of DC-CPin7 and CBP bromodomain

To accurately illustrate the binding mode of **DC-CPin7** and to depict its interactions with

CBP bromodomain, we determined the X-ray crystal structure of the CBP bromodomain (amino

acids 1,082–1,197) in complex with **DC-CPin7**, at 2.46 Å resolution (Figure 2, data collection

shown in Table 1). The inhibitor was well defined by its electron density facilitating the mapping
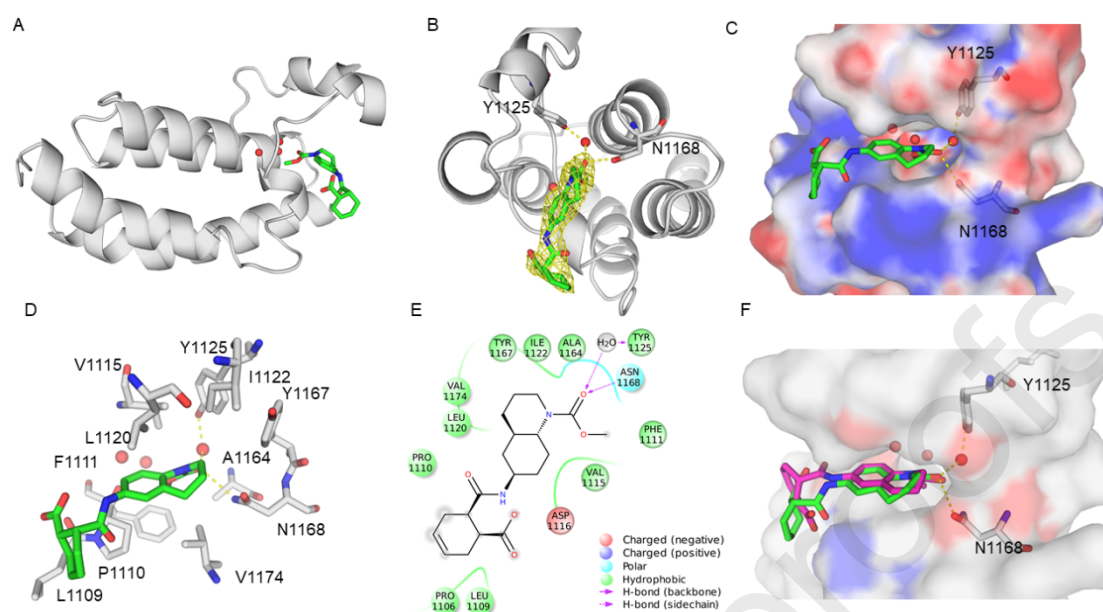
of its binding mode.

Figure 2. The binding mode of **DC-CPin7** to CBP bromodomain. (A) The X-ray crystal structure of the CBP bromodomain (amino acids 1,082–1,197) in complex with **DC-CPin7** (PDB code 6LQX). (B) Enlarged view of the **DC-CPin7** binding site in the CBP bromodomain in cartoon animation. The $2F_o-F_c$ electron density map calculated at 2.46 Å for **DC-CPin7** is contoured at 1σ. (C) Enlarged view of **DC-CPin7** interacting with the electrostatic surface of CBP bromodomain generated by APBS tools. (D) The 3D interaction map between **DC-CPin7** and representative residues around 4 Å. (E) The 2D interaction map between **DC-CPin7** and representative residues around 4 Å generated by Maestro. (F) The coordinate alignment of DC-CPin7 in co-crystal (green) with DC-CPin7 in docking result (purple).

As shown in the interaction maps of **DC-CPin7** and CBP bromodomain (Figure 2B-2E), as expected, the N-methoxycarbonyl at the head of **DC-CPin7** binds in the KAc (acetylated lysine) binding site. The amide carbonyl at the head makes a direct hydrogen bond to Asn1168 and an additional water-mediated hydrogen bond to Tyr1125. The several water molecules sitting in the binding pocket were also consistent with previous bromodomain crystal structures[20]. Meanwhile, the tail of **DC-CPin7** lies near a hydrophobic pocket formed by Leu1109, Pro1110 and Phe1111, and the cyclohexene ring makes van der Waals interactions with Pro1110.Notably, the binding mode of DC-CPin7 observed in the co-crystal structure was successfully predicted in

our *in silico* screening docking result (Figure 2F).
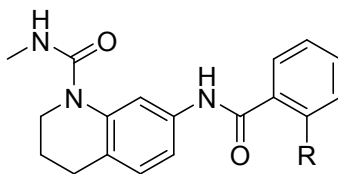
Table 1. Data collection and refinement statistics.

Wavelength	0.9785
Resolution range	34.39 - 2.46 (2.548 - 2.46)
Space group	P 1 21 1
Unit cell	44.89 68.789 76.669 90 91.748 90
Total reflections	116080
Unique reflections	16809 (1643)
Completeness (%)	98.36 (97.33)
Mean I/sigma(I)	2.500
Wilson B-factor	26.29
R-merge	0.117
CC1/2	0.879
Reflections used in refinement	16808 (1643)
Reflections used for R-free	784 (57)
R-work	0.1701 (0.2302)
R-free	0.2607 (0.3392)
Number of non-hydrogen atoms	4054
macromolecules	3838
ligands	32
solvent	184
Protein residues	455
RMS(bonds)	0.009
RMS(angles)	1.23
Ramachandran favored (%)	97.54
Ramachandran allowed (%)	2.24
Ramachandran outliers (%)	0.22
Rotamer outliers (%)	2.78
Clashscore	13.18
Average B-factor	28.67
macromolecules	28.57
ligands	39.06
solvent	29.05

Statistics for the highest-resolution shell are shown in parentheses.

2.3 Chemical modification of DC-CPin7

From the co-crystal structure of **DC-CPin7**, we found two areas in the binding site that could further improve potency: the head in the KAc binding site and the tail near the hydrophobic regions. First, we successfully obtained compound **DC-CPin701** by replacing N-methoxycarbonyl with N-methylurea to reinforce electrostatic interactions, meanwhile replacing the 6- position cyclohexene with 7- position phenyl ring to enhance hydrophobic interactions and molecular rigidity. It turned out the inhibitory potency of **DC-CPin701** was slightly increased. Next, we focused on optimization of the tail. Our hypothesis for improving potency of **DC-CPin701** was substituting benzoic acid with benzamide at benzene ring (Table 2), which might increase hydrophobic interactions with Pro1110. Apparently, benzamide substituents were more potent than **DC-CPin701** might be the result of van der Waals interactions between amide and Pro1110. Meanwhile, extension of the methyl substituent of compound **DC-CPin702** to isopropyl (**DC-CPin706**) resulted in 4-fold increase in potency, which most likely was due to the increased van der Waals interaction of the propyl substituent with an additional residue Val1109. Though molecular docking analysis, we found that the urea moiety of **DC-CPin706** was deeper into the KAc binding pocket and closer to Asn1168 and the water molecule than the carboxylate moiety of **DC-CPin7**, so that the urea group could form several strong hydrogen bonds. The tail lay in the hydrophobic pocket, and sandwiched between Leu1120 and Pro1110, making van der Waals interactions with Leu1109, Pro1110 and Leu1120.

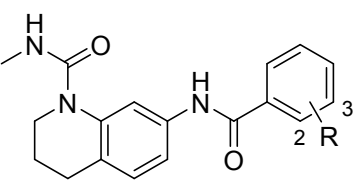**Table 2. The inhibitory activities of benzamide derivatives based on DC-CPin701**

Compound	R	IC_{50} $(\mu M)^a$
DC-CPin701	COOH	2.48
DC-CPin702	$CONHCH_3$	0.778
DC-CPin703	$CON(CH_3)_2$	0.936
DC-CPin704	$CONHCH_2CH_3$	0.410
DC-CPin705	$CONHCH_2CH_2CH_3$	0.482
DC-CPin706	$CONHCH(CH_3)_2$	0.223

[a] All IC_{50} values are reported as means of values from at least two determinations.

Next, we replaced the amide group with phenyl ring at the 2- or 3- position (Table 3) to determine the most suitable location in the hydrophobic pocket and improve molecular rigidity which could restrict internal rotation of the tail. Compound **DC-CPin707** showed the same inhibitory potency compared to **DC-CPin706**, which was better than all the amide derivatives synthesized previously. However, compound **DC-CPin708** gave a dramatic loss in potency

compared to **DC-CPin707**, revealing that residues of the hydrophobic pocket might clash with

2-position derivatives which occupied as much space as the phenyl ring.

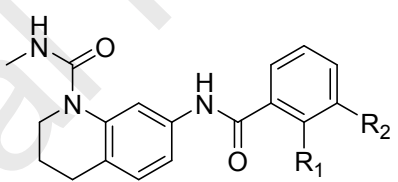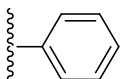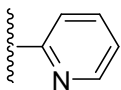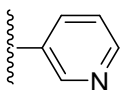**Table 3. The inhibitory activities of phenyl substituted derivatives**

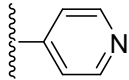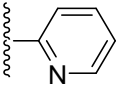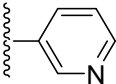| Compound	R	IC_{50} (μM)[a]
DC-CPin706	2-CONHCH(CH_3)$_2$	0.223
DC-CPin707	3-Ph	0.213
DC-CPin708	2-Ph	8.41
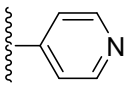
[a] All IC_{50} values are reported as means of values from at least two determinations.

We raised a hypothesis that the tail sitting in the hydrophobic pocket could form a hydrogen

bond with residues around the hydrophobic pocket, which might increase binding affinity and

selectivity. Various pyridyl analogues at the 2- or 3-position (Table 4) were synthesized to further

explore the hydrophobic pocket and support our hypothesis. It turned out that almost all

substituents had an increase in inhibitory potency compared to **DC-CPin707**. However, we

noticed that **DC-CPin714** lost inhibitory potency which had comparable potency to **DC-CPin708**,

further validated our hypothesis. Generally, moving the pyridine from the 2-position to the

3-position resulted in a good increase in inhibitory potency, which was likely because the pyridyl

moiety at the 3-position was more suitable in the hydrophobic pocket. Importantly, **DC-CPin711**

garnered our attention for its strong potency compared to other heterocyclic derivatives

(approximately 3-fold potency over **DC-CPin707**). Modeling analysis of **DC-CPin711** (Figure 3E

and 3F) showed that N-methylurea moiety occupied the KAc binding site, making multiple

hydrogen bonds with Asn1168, Pro1110 and Tyr1125. The tail of **DC-CPin711** was sandwiched

between Val1174 and Leu1109, while the phenyl ring and pyridyl ring made van der Waals

interactions with the hydrophobic pocket formed by Leu1109 and Pro1110. The pyridine ring sat

in the hydrophobic pocket where nitrogen atom made a hydrogen bond with Arg1173 and formed

a π stacking interactions with the pyrrolidinyl moiety of Pro1110. Taken together, the docking

results rationalized the SAR and established a reasonable binding mode for further structural

modification.

Table 4. The inhibitory activities of pyridyl analogues DC-CPin707-DC-CPin714

Compound	R_1	R_2	IC_{50} (μM)[a]
DC-CPin707	H		0.213
DC-CPin709	H		0.103
DC-CPin710	H		0.106

DC-CPin711	H			0.0626
DC-CPin712		H		0.105
DC-CPin713		H		0.485
DC-CPin714		H		5.08

[a] All IC_{50} values are reported as means of values from at least two determinations.

Chemistry. Compound **DC_3** was prepared as depicted in Scheme 1. Treatment of tetrahydroquinoline **1** with chloroformate **2** yielded **DC_1**, then followed by methylamine hydrochloride produced urea **DC_2**. Hydrogenation of **DC_2** afforded key intermediate **DC_3** from which all the compounds were formed.
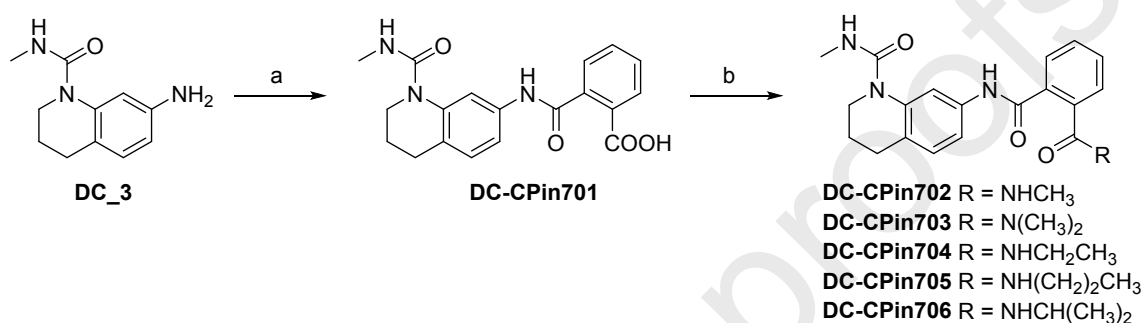
Scheme 1. Synthesis of Key Intermediate DC_3.
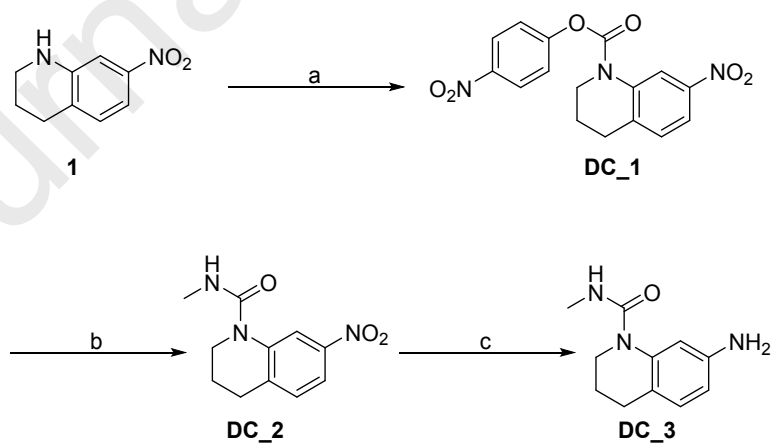
Reagents and conditions: (a) 4-nitrophenyl chloroformate, TEA, DCM, 0 ℃; (b) methylamine hydrochloride, K_2CO_3, MeCN, 60 ℃; (c) H_2, Pd/C, MeOH, rt.

Scheme 2 shows key intermediate **DC_3** was used to produce compounds **DC-CPin701** to

DC-CPin706. Treatment of amine **DC_3** with phthalic anhydride afforded acid **DC-CPin701**, and

compounds **DC-CPin702** to **DC-CPin706** could be accessed with amide coupling of appropriate

amine.

Scheme 2. Synthesis of Compounds DC-CPin701-DC-CPin706.

DC_3   **DC-CPin701**

DC-CPin702 R = NHCH$_3$
DC-CPin703 R = N(CH$_3$)$_2$
DC-CPin704 R = NHCH$_2$CH$_3$
DC-CPin705 R = NH(CH$_2$)$_2$CH$_3$
DC-CPin706 R = NHCH(CH$_3$)$_2$

Reagents and conditions: (a) phthalic anhydride, THF, rt; (b) amine, DIPEA, HATU, DCM, rt.

Amide coupling of **DC_3** with 3-biphenylcarboxylic or 2-biphenylcarboxylic acid provided

DC-CPin707 and **DC-CPin708** in Scheme 3.

Scheme 3. Synthesis of Compounds DC-CPin707 and DC-CPin708.

DC_3

DC-CPin707 R = 3-Ph
DC-CPin708 R = 2-Ph
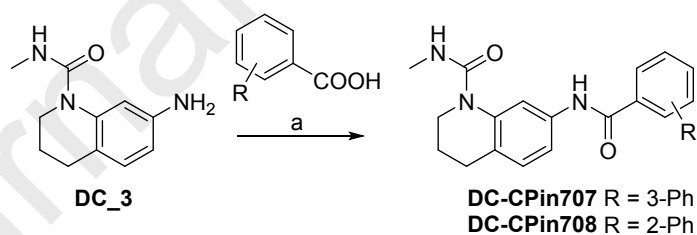
Reagents and conditions: (a) DIPEA, HATU, DCM, rt.

The synthesis of aryl analogues **DC-CPin709** to **DC-CPin714** is outlined in Scheme 4. Acids

DC_4 to **DC_9** were formed from Suzuki coupling of 3-Carboxyphenylboronic acid **11** or

2-Carboxyphenylboronic **12** acid with appropriate aryl bromides. Subsequent amide coupling with

intermediate **DC_3** yielded **DC-CPin709** to **DC-CPin714.**

Scheme 4. Synthesis of Compounds DC-CPin709-DC-CPin714.

11 (3-B(OH)₂)
12 (2-B(OH)₂)

DC_4 R = 3-(2-pyridyl)
DC_5 R = 3-(3-pyridyl)
DC_6 R = 3-(4-pyridyl)
DC_7 R = 2-(2-pyridyl)
DC_8 R = 2-(3-pyridyl)
DC_9 R = 2-(4-pyridyl)

DC-CPin709 R = 3-(2-pyridyl)
DC-CPin710 R = 3-(3-pyridyl)
DC-CPin711 R = 3-(4-pyridyl)
DC-CPin712 R = 2-(2-pyridyl)
DC-CPin713 R = 2-(3-pyridyl)
DC-CPin714 R = 2-(4-pyridyl)
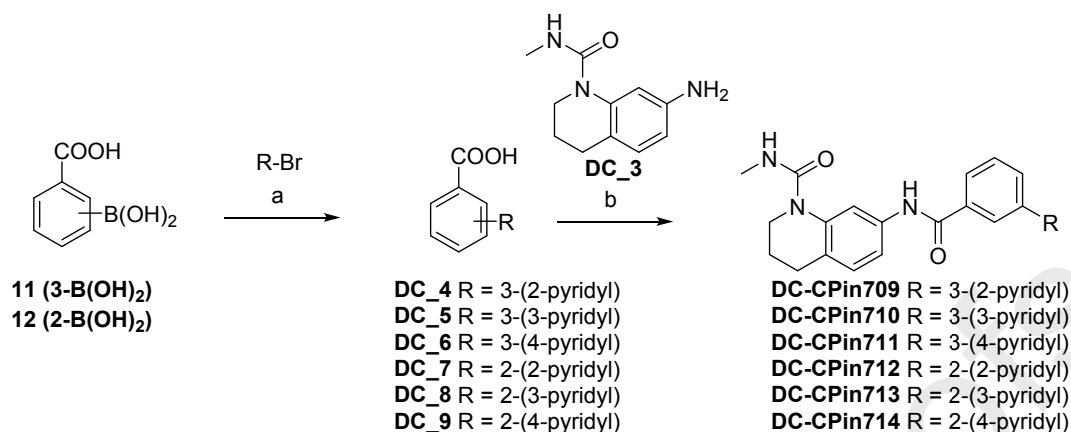
Reagents and conditions: (a) DME/ water, Na_2CO_3, Pd(dppf)Cl₂, 100 °C; (b) DIPEA, HATU, DCM, rt.

2.4 *In vitro* activity of DC-CPin711

The *in vitro* activities of **DC-CPin7** derivatives were measured by HTRF as previously, among which **DC-CPin711** showed the greatest potency with the IC_{50} value of 63.3 ± 4.0 nM, while **DC-CPin708** was the weakest derivative with the IC_{50} value of 8.4 ± 0.9 μM (Figure 3A),which was selected as negative compound facilitating to prove the on-target effects of drug of interest. To further validate the direct binding of **DC-CPin711**, we preformed CPMG and STD NMR experiments to validate direct binding of **DC-CPin711** to CBP bromodomain, the results were included in Supplementary Figure 3. Furthermore, microscale thermophoresis (MST) experiments were used to measure the K_d value of **DC-CPin711** with CBP bromodomain. The K_d value calculated by a K_d fitting model of microscale thermophoresis trace of **DC-CPin711** bound to CBP bromodomain was 74.4 nM (Figure 3C), which confirmed the strong interactions between **DC-CPin711** and CBP bromodomain. Besides, we utilize molecular docking to obtain its 3D and 2D interaction map with CBP bromodomain

(Figure 3D and 3E). The binding mode of **DC-CPin711** has been discussed in chemical optimization section. The selectivity of CBP inhibitors has become an important issue of current non-BET family bromodomain inhibitor development. Hereby, ALPHAScreen assays were adopted to test the inhibitory activities of **DC-CPin711 to** BRD4 bromodomains.The result showed that **DC-CPin711** showed over 150-fold selectivity to BRD4 bromodomains(Figure 3F). Previous molecular molecular dynamics and metadynamics simulations suggested that Arg1173, as the unique residue for CBP, may be responsible for the selective binding[21], which indicate the selectivity of **DC-CPin711** may partly due to the hydrogen bond between pyridine of **DC-CPin711** and Arg1173.
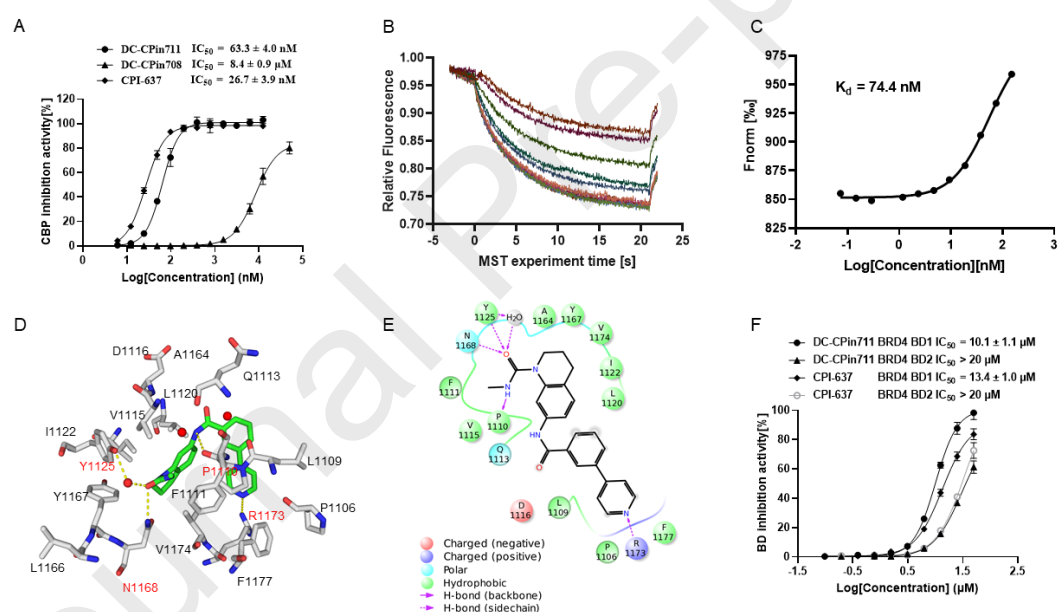

Figure 3. The *in vitro* activity of DC-CPin711. (A) The IC_{50} curve of DC-CPin711 against CBP bromodomain tested by HTRF. CPI-637 was used as positive control. (B) Microscale thermophoresis trace of DC-CPin711 binding to CBP bromodomain. (C) The K_d fitting curve of DC-CPin711 binding to CBP bromodomain using K_d fitting model. (D) The 3D interaction map between DC-CPin711 and representative residues around 4 Å (E) The 2D interaction map between DC-CPin711 and representative residues around 4 Å generated by Maestro. (F) The inhibitory activities of DC-CPin711 on two BRD4 bromodomains.CPI-637 was used as positive control.

2.5 Cellular activity of DC-CPin711

Since CBP is involved in the etiology and progression in varieties of human cancers, we evaluated the cell proliferation inhibitory activities of **DC-CPin711** across 12 cancer cell lines for 96h (Table 5 and Supplementary Figure 4). The broadest sensitivity was observed in hematological malignancies, where **DC-CPin711** exhibited potent inhibitory activities against all acute myeloid leukemia cell lines tested, among which MV4-11 cells were the most sensitive cancer cells with an IC_{50} value of 1.2 μM. By contrast, many solid tumor cell lines tested including renal cancer, pancreatic cancer, lung cancer, triple-negative breast cancer and androgen receptor-negative prostate cancer were insensitive to **DC-CPin711** except that androgen receptor-positive prostate cancer cells (22Rv-1 cell line) were also sensitive with a IC_{50} value of 13.0 μM. These anti-proliferation activities tested were in accordance with previous reported results[13, 22, 23]. We also investigated the cell proliferation inhibition of negative compound **DC-CPin708** in MV4-11 cell line, which turned out to show little anti-proliferation effects in MV4-11 cell line (Figure 4A). Moreover, the cytotoxicity of **DC-CPin711** to HUVEC and MRC-5 normal cell lines was also inspected. Barely any inhibition was observed in these two normal cell lines (Figure 4B and 4C). We chose the most sensitive cell line MV4-11 cell line to study its anti-tumor mechanism. Previous studies have shown that inhibition of the CBP bromodomain could regulate the expression level of c-Myc and thus alters cell cycle , cell apoptosis and metabolism[5, 6, 24]. Western blot analysis was been used to detect the changes of c-Myc expression levels after treatment of **DC-CPin711** (0, 1.25, 2.5, 5, 10 μM) for 48h. As evidenced in figure 4D, **DC-CPin711** was able to significantly decrease c-Myc expression levels at a dose-dependent manner in MV4-11 cells,

the densitometric result was also provide in Figure 4E. Considering the significant inhibition of

c-Myc expression by **DC-CPin711**, we investigated the potential mechanism of **DC-CPin711**

induced MV4-11 cell proliferation inhibition. To this end, MV4-11 cells were exposed to

different concentrations of **DC-CPin711** (0, 1.25, 5, 10 μM). Cell cycle distribution was then

determined by flow cytometry after 48h of treatment. DC-CPin711 significantly arrested cell

cycle progression at G1 phase (Figure 4F and Supplementary Figure 5A). Exposure to 10 μM

of **DC-CPin711** arrested 73.3% of the MV4-11cells in G1 phase, compared with 53.1% in

control cells. We then continued to evaluate the effects of **DC-CPin711** on MV4-11 cells. As

shown in Figure 4F, **DC-CPin711** induced dose-dependent apoptosis in MV4-11 cells: 35.7%

of MV4-11 cells after 96h treatment of 10 μM of **DC-CPin711** were apoptotic, while the

untreated control cells were 1.3% (Supplementary Figure 5B). These results demonstrated

that **DC-CPin711** as a novel CBP bromodomain inhibitor could induce G1 phase cell cycle

arrest and cell apoptosis, thereby inhibiting the proliferation of MV4-11 acute myeloid

leukemia cells.

Table 5. Cell proliferation inhibition IC$_{50}$ of DC-CPin711

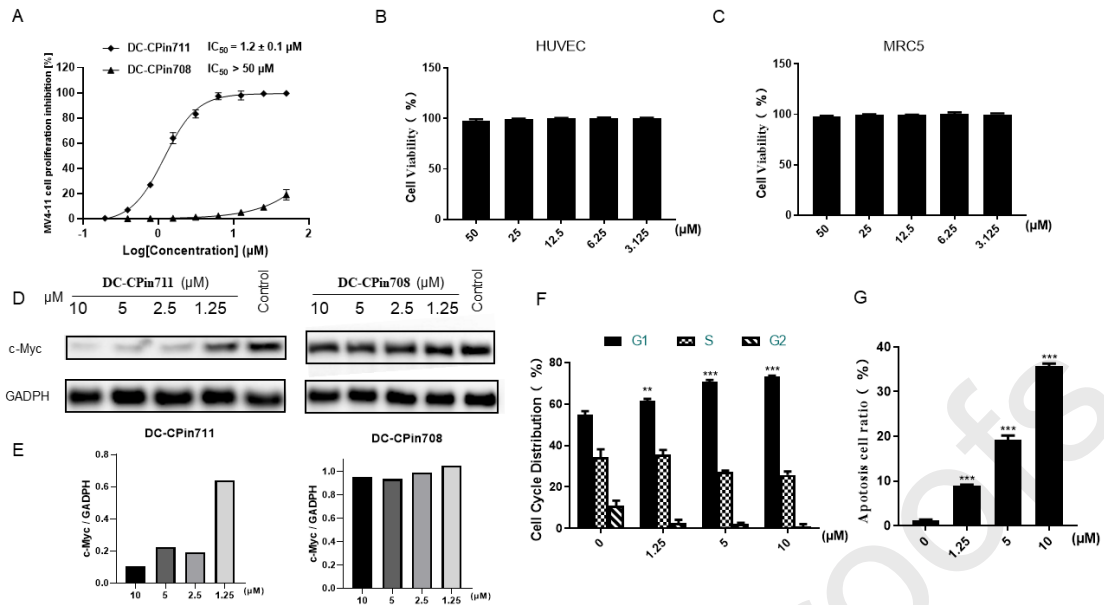| Cell	MDA-MB-231	DU-145	22RV-1	Panc-1	PC-9	786-O	Jurkat	DHL-4	KMS 12	THP -1	Kasumi-1	MV4 -11
IC$_{50}$ （μM）	>30	>30	13.0	>30	>30	>30	19.5	4.9	1.7	3.9	2.5	1.2

Figure 4. Cellular activity of DC-CPin711 on MV4-11 cells. (A) The cell proliferation inhibition of DC-CPin711 and negative compound DC-CPin708 on MV4-11 cells for 96h. (B-C) Normalized cell viability of HUVEC and MRC5 cells after 96h of DC-CPin711 treatment using DMSO control. (D) The c-Myc protein expression levels after 48h of DC-CPin711 or DC-CPin708 treatment. (E)The normalized densitometry analysis of figure 4E using ImageJ software, DMSO control was used to normalize the relative density. (F) The cell cycle alterations of MV4-11 cells after 48h of DC-CPin711 treatment. (G) The cell apoptosis changes of MV4-11 cells after 96h of DC-CPin711 treatment. （**$P < 0.01$， ***$P < 0.001$ as compared with control cells）

3.Conclusion

Herein by the means of *in silico* screening **DC-CPin7** was been identified as a hit, which showed micromolar potency toward CBP bromodomain. A series of biochemical and biophysical experiments validated the direct binding of the hit to CBP bromodomain. The co-crystal of CBP bromodomain in complex with **DC-CPin7** we obtained guided the rational drug design of CBP bromodomain inhibitors targeting KAc binding site and the hydrophobic pocket. With the replacement of the urea group in the head, we focused on modifications in the tail. We optimized the tail from benzamide derivatives to pyridyl substituents and eventually managed to obtain **DC-CPin711** with the IC_{50} value of 63.3 ± 4.0 nM, displaying approximately 40-fold potency over **DC-CPin7** with the IC_{50} value of 2.5 ± 0.3 μM. Notably, **DC-CPin711** showed over 150-fold selectivity to BRD4 bromodomains. Moreover, **DC-CPin711** showed moderate anti-leukemia and anti-AR-positive prostate cancer cells effects. The discovery of **DC-CPin711** may serve as a reliable lead compound to guide further optimization of hydrophobic pocket occupying tail and facilitate the development of potent and selective CBP bromodomain inhibitors, which may be utilized as potential potent anti-leukemia and anti-AR-positive prostate cancer drugs. These results demonstrated how *in silico* screening and molecular docking cooperating with rational chemical optimization could play a significant role in the drug discovery and development progress.

4.Experimental Section

4.1 Chemistry

4.1.1 General Methods.

Unless otherwise stated, all solvents and reagents were used as obtained. All products were confirmed by NMR spectra and high-resolution mass spectra. NMR analysis was performed in a deuterated solvent with a Bruker Avance 400 MHz or Varian Inova 400 MHz or Bruker Avance 600 MHz spectrometer referenced to trimethylsilane. Proton coupling patterns were described as broad (b), singlet (s), doublet (d), triplet (t), quartet (q), multiplet (m) and all coupling constants (*J* values) are reported in hertz (Hz). Mass spectra were measured with a triple TOF 5600+ MS/MS system (AB Sciex, Concord, Ontario, Canada) in the negative or positive ESI mode. Reactions were monitored by thin-layer chromatography (UV detection at 254 nm) or UPLC-MS (Waters Acquity UPLC H-class with Waters SQ Detector 2) analysis. Column chromatography was performed on silica gel (200-300 mesh). All tested compounds were purified to ≥95% purity as determined by ultra-performance liquid chromatography (UPLC). The following analytical method was used to determine chemical purity of final compounds: Waters UPLC H-Class with ACQUITY UPLC BEH C18 reversed-phase column (2.1 mm × 50 mm, 1.7 μm, flow rate = 0.5 mL/min). Mass analysis was performed by waters SQD2 single quadrupole mass detection system.

4.1.2 Synthesis and Characterization of 7-amino-N-methyl-3,4-dihydroquinoline-1(2H)-carboxamide (DC_3). *Step 1: 4-nitrophenyl 7-nitro-3,4-dihydroquinoline-1(2H)-carboxylate (DC_1)*. To a solution of 7-nitro-1,2,3,4-tetrahydroquinoline (4 g, 22.45 mmol) in anhydrous DCM (50 mL) was added dry

TEA (6 mL, 43.17 mmol) and 4-nitrophenyl chloroformate (5 g, 24.81 mmol) carefully at 0°C, the resulting mixture was then stirred at room temperature for 12 h. The solvent was removed under reduced pressure and the crude product was purified by column chromatography (petroleum ether/EtOAc = 5:1) to obtain the title compound (**DC_1**, 5.526 g, 72%) as a red oil. LCMS *m/z* (M + H) 344.

*Step 2: N-methyl-7-nitro-3,4-dihydroquinoline-1(2H)-carboxamide (**DC_2**)*. To a solution of 4-nitrophenyl 7-nitro-3,4-dihydroquinoline-1(2H)-carboxylate (**DC_1**, 5.526 g, 16.1 mmol) in MeCN (50 mL) was added methylamine hydrochloride (2.174 g, 32.2 mmol) and K_2CO_3 (6.675g, 48.3 mmol). The mixture was stirred at 60°C for 6 h and cooled to room temperature, then filtered and evaporated to dryness. The residue was purified by column chromatography (DCM/MeOH = 40:1) to yield the title compound (**DC_2**, 3.106 g, 82%) as a pale yellow solid. ^{1}H NMR (400 MHz, Chloroform-*d*) δ 8.34 (d, *J* = 2.4 Hz, 1H), 7.87 – 7.81 (m, 1H), 7.26 (d, *J* = 8.2 Hz, 1H), 4.98 (s, 1H), 3.74 (t, *J* = 6.0 Hz, 2H), 2.90 (d, *J* = 4.8 Hz, 3H), 2.82 (t, *J* = 6.5 Hz, 2H), 1.98 (p, *J* = 6.1 Hz, 2H). LCMS *m/z* (M + H) 236.

*Step 3: 7-amino-N-methyl-3,4-dihydroquinoline-1(2H)-carboxamide (**DC_3**)*. N-methyl-7-nitro-3,4-dihydroquinoline-1(2H)-carboxamide (**DC_2**, 3.106 g, 13.2 mmol) and 10% Pd/C (3.106 g) were added in methanol (20 mL). The mixture was stirred at room temperature under H_2 atmosphere for 6 h. The mixture was filtered by using Celite and concentrated *in vacuo*. The residue was purified by column chromatography (DCM/MeOH = 30:1) to produce the title compound (**DC_3**, 1.855 g, 68%) as a brown oil. ^{1}H NMR (600 MHz, Chloroform-*d*) δ 6.92 (d, *J* = 8.0 Hz, 1H), 6.61 (d, *J* = 2.4 Hz, 1H), 6.42 (dd, *J* = 2.4, 8.1 Hz, 1H), 5.26 (s, 1H), 3.71 (t, *J* = 6.1 Hz, 2H), 2.99 (s, 2H), 2.82 (d, *J* = 4.7 Hz, 3H), 2.63 (t, *J* = 6.8 Hz, 2H), 1.86 (d, *J* = 6.1 Hz,

2H). LCMS *m/z* (M + H) 206.

4.1.3 **Syntheis** **and** **Characterization** **of** **N¹-methyl-N²-(1-(methylcarbamoyl)-1,2,3,4-tetrahydroquinolin-7-yl)phthalamide** **(DC-CPin702).** *Step* *1:* *2-((1-(methylcarbamoyl)-1,2,3,4-tetrahydroquinolin-7-yl)carbamoyl)benzoic acid (DC-CPin701).* To a solution of 7-amino-N-methyl-3,4-dihydroquinoline-1(2H)-carboxamide (**DC_3**, 411 mg, 2 mmol) in THF (5 mL) was added phthalic anhydride (444 mg, 3 mmol). The residue was stirred at rt for 3 h, then concentrated *in vacuo*. The crude product was purified by column chromatography (DCM/MeOH = 10:1) to yield the title compound (**DC-CPin701**, 643 mg, 91%) as a brown solid. ¹H NMR (400 MHz, Methanol-d_4) δ 8.05 (d, *J* = 7.7 Hz, 1H), 7.73 – 7.64 (m, 2H), 7.62 – 7.56 (m, 2H), 7.32 – 7.26 (m, 1H), 7.15 (d, *J* = 8.2 Hz, 1H), 3.70 (t, *J* = 6.2 Hz, 2H), 2.80 (s, 3H), 2.77 (t, *J* = 6.6 Hz, 2H), 1.94 (p, *J* = 6.4 Hz, 2H). LCMS *m/z* (M + H) 354. HRMS *m/z* 354.1452 (M + H⁺, $C_{19}H_{19}N_3O_4$, requires 354.1448).

Step 2: N¹-methyl-N²-(1-(methylcarbamoyl)-1,2,3,4-tetrahydroquinolin-7-yl)phthalamide (DC-CPin702). To a solution of 2-((1-(methylcarbamoyl)-1,2,3,4-tetrahydroquinolin-7-yl)carbamoyl)benzoic acid (**DC-CPin702,** 35 mg, 0.1 mmol) in DCM (5 mL) was added O-(7-azabenzotriazol-1-yl)-N,N,N',N'-tetramethyluronium hexafluorophosphate (HATU, 57 mg, 0.15 mmol), N,N-diisopropylethylamine (DIPEA, 39 mg, 0.3 mmol) and stirred at rt for 0.5 h before methylamine hydrochloride (14 mg, 0.2 mmol) was added. The mixture was stirred for 2 h at rt and concentrated to dryness. The crude residue was purified by silica gel chromatography (DCM/MeOH = 20:1) to give the title compound (**DC-CPin702**, 24 mg, 65%) as a pale yellow

solid. ^{1}H NMR (400 MHz, Methanol-d_4) δ 7.88 – 7.84 (m, 1H), 7.70 (d, J = 2.1 Hz, 1H), 7.68 –

7.64 (m, 1H), 7.61 – 7.58 (m, 2H), 7.30 (dd, J = 2.1, 8.2 Hz, 1H), 7.14 (d, J = 8.2 Hz, 1H), 3.69 (t,

J = 6.1 Hz, 2H), 2.90 (s, 3H), 2.80 (s, 3H), 2.75 (t, J = 6.6 Hz, 2H), 1.93 (p, J = 6.6 Hz, 2H).

LCMS m/z (M + H) 367. HRMS m/z 389.1583 (M + Na$^+$, $C_{20}H_{22}N_4O_3$, requires 389.1584).

4.1.4 **Syntheis** **and** **Characterization** **of**

7-([1,1'-biphenyl]-3-carboxamido)-N-methyl-3,4-dihydroquinoline-1(2H)-carboxamide

(DC-CPin707). To a solution of 3-biphenylcarboxylic acid (40 mg, 0.2 mmol) in DCM (5 mL)

was added *O*-(7-azabenzotriazol-1-yl)-*N,N,N′,N′*-tetramethyluronium hexafluorophosphate

(HATU, 114 mg, 0.3 mmol), *N,N*-diisopropylethylamine (DIPEA, 78 mg, 0.6 mmol), then stirred

at rt for 0.5 h before 7-amino-N-methyl-3,4-dihydroquinoline-1(2H)-carboxamide (**DC_3**, 42 mg,

0.2 mmol) was added. The mixture was stirred at room temperature for 3 h and concentrated *in*

vacuo. The crude residue was purified by silica gel chromatography (DCM/MeOH = 25:1) to give

the title compound (**DC-CPin707**, 38 mg, 49%) as a yellow solid. ^{1}H NMR (600 MHz,

Methanol-d_4) δ 8.17 (t, J = 1.9 Hz, 1H), 7.90 (d, J = 7.8 Hz, 1H), 7.84 (d, J = 8.3 Hz, 1H), 7.73 (d,

J = 2.1 Hz, 1H), 7.70 (d, J = 7.2 Hz, 2H), 7.59 (t, J = 7.7 Hz, 1H), 7.47 (t, J = 7.7 Hz, 2H), 7.38 (t,

J = 7.4 Hz, 1H), 7.34 (dd, J = 2.1, 8.2 Hz, 1H), 7.14 (d, J = 8.2 Hz, 1H), 3.65 (t, J = 6.2 Hz, 2H),

2.80 (s, 3H), 2.72 (t, J = 6.6 Hz, 2H), 1.91 (p, J = 6.4 Hz, 2H). LCMS m/z (M + H) 386. HRMS

m/z 386.1866 (M + H$^+$, $C_{24}H_{23}N_3O_2$, requires 386.1863).

4.1.5 **Synthesis** **and** **Characterization** **of**

N-methyl-7-(3-(pyridin-2-yl)benzamido)-3,4-dihydroquinoline-1(2H)-carboxamide

(DC-CPin709). *Step 1: 3-(pyridin-2-yl)benzoic acid (**DC_4**)*. To a solution of 2-bromopyridine

(166 mg, 1 mmol) in DME (12 mL) and 2N Na_2CO_3 (4 mL) was added 3-Carboxyphenylboronic

acid (237 mg, 1.5 mmol), [1,1'-bis(diphenylphosphino)ferrocene]-dichloropalladium(II) (73 mg,

0.1 mmol). The reaction mixture was protected by N_2 and heated to 100 °C for 4 h. The mixture

was then cooled to rt, filtered and concentrated *in vacuo*. The residue was purified by silica gel

chromatography (DCM/MeOH = 20:1) to produce the title compound (**DC_4**, 148 mg, 74%) as a

colorless oil. LCMS *m/z* (M + H) 200.

*Step 2: N-methyl-7-(3-(pyridin-2-yl)benzamido)-3,4-dihydroquinoline-1(2H)-carboxamide
(DC-CPin709)*. In a similar procedure to **DC-CPin707**, compound **DC-CPin709** was prepared

from 3-(pyridin-2-yl)benzoic acid (**DC_4**, 40 mg, 0.2 mmol) and

7-amino-N-methyl-3,4-dihydroquinoline-1(2H)-carboxamide (**DC_3**, 42 mg, 0.2 mmol). The

crude residue was purified by silica gel chromatography (DCM/MeOH = 50:1) to give the title

compound (**DC-CPin709**, 34 mg, 44%) as a yellow oil. ^{1}H NMR (400 MHz, Chloroform-*d*) δ 8.87

(d, *J* = 11.1 Hz, 1H), 8.68 (d, *J* = 4.8 Hz, 1H), 8.51 (t, *J* = 1.9 Hz, 1H), 8.10 (d, *J* = 7.8 Hz, 1H),

7.99 (d, *J* = 7.7 Hz, 1H), 7.87 – 7.80 (m, 2H), 7.71 (d, *J* = 2.0 Hz, 1H), 7.58 (t, *J* = 7.8 Hz, 1H),

7.35 – 7.29 (m, 2H), 7.10 (d, *J* = 8.3 Hz, 1H), 5.59 (d, *J* = 4.9 Hz, 1H), 3.78 – 3.62 (m, 3H), 2.85

(d, *J* = 4.6 Hz, 3H), 2.71 (t, *J* = 6.6 Hz, 2H), 1.90 (p, *J* = 6.3 Hz, 2H). LCMS *m/z* (M + H) 387.

HRMS *m/z* 387.1808 (M + H$^+$, $C_{23}H_{22}N_4O_2$, requires 387.1816).

4.2 Structure-based *in silico* screening

The in-house small molecule compounds database containing approximately 364,000

compounds was prepared by Maestro (Maestro, version 9.1; Schrödinger, LLC: New York, 2010)

Ligand Preparation module was used to generate ionized 3D low-energy conformations in pH

range of 7.4 ± 2.0. The crystal structure of CBP bromodomain (PDB Code: 4OUF) was prepared

by Protein Preparation module with standard protocols. The receptor grid was defined as the enclosing box centered at crucial residue N1168 with the box size of 20.0 Å. Then molecular docking-based *in silico* screen was finished at the glide standard precision (SP) mode with flexible ligand sampling. Top 1000 candidates were picked out for cluster analysis using Pipeline Pilot (Pipeline Pilot, version 7.5, Accelrys Software Inc.).

4.3 Biology

4.3.1 Protein Expression and Purification

The DNA fragment encoding CBP bromodomain (residue 1082-1197) was cloned in a glutathione S-transferase tag-containing pGEX-6p-1 vector. The desired protein was overexpressed in *E. coli* BL21 (DE3) cells after inducing overnight at 16 °C using 0.4 mM isopropyl β-D-1-thiogalactopyranoside (IPTG). Cells were collected and then resuspended and sonicated in buffer A (20 mM HEPES, pH 7.4, 100 mM NaCl). The supernatant was loaded onto the GST affinity column (GE Healthcare) after ultracentrifugation. The recombinant CBP bromodomain proteins were eluted with buffer B (20 mM HEPES, pH 7.4, 100 mM NaCl and 20 mM reduced L-glutathione), and were further purified by molecular size exclusion chromatography using a Superdex 75 10/300GL column (GE Healthcare) in 25 mM HEPES, pH 7.4, 150 mM NaCl. Protein-containing fractions were combined, concentrated, and stored at -80 °C for further experiments.

4.3.2 Homogeneous time resolved fluorescence assay

The final volume of reaction is 20 μL. All components in this assay were diluted in a buffer of 20 mM HEPES pH 7.4 , 150 mM NaCl, 0.1% bovine serum albumin (w/v), 0.01%Triton

X-100(v/v), and then 5μL of compound solution were transferred to 384-well plates (PerkinElmer). Add 2.5ul of GST-CBP bromodomain protein with a final concentration of 10nM to a 384-well plate and react with compounds for 30min at room temperature. Then, add 2.5ul of tetra-acetylated substrate peptide [SGRG-K (Ac) -GG-K (Ac)-GLG-K (Ac) -GGA-K (Ac) -RHRKVGG-K (biotin)] (ChinaPeptides) with a final concentration of 100nM and incubate at room temperature for 30min. Finally add 10ul of a mixed solution of two HTRF fluorophores beads (Anti GST-Eu cryptate donor beads and Streptavadin-XL665 acceptor beads (Cisbio, Cat# 61GSTKLB and 610SAXLB)) and 800mM KF and incubate for 90min. After stopping reaction, the fluorescence signal was detected and collected by EnVision microplate reader (PerkinElmer, LANCE/DELFIA Dual/Bias mirror, Eu ex 337 nm, Eu em 615 nm; XL665 em 665/10 nm). Finally, the results were calculated by GraphPad Prism 6.0.

4.3.3 Protein Thermal Shift Assay

CBP bromodomain protein mixed with SYPRO Orange Dye (Sigma-Aldrich, S5692) was diluted to 5 μM in the assay buffer (25mM PIPES pH 6.2, 150mM NaCl) and transferred to assay plates. Then different concentrations of compounds or 1 μL DMSO were added to the protein assay solution. Quant Studio 6 Flex Real-Time PCR system (Applied Biosystems) was been used to test the protein stabilization of all samples. Following calculation of thermal shift values were finished by protein thermal shift software (version 1.3, Applied Biosystems).

4.3.4 Nuclear Magnetic Resonance Experiments

Bruker AVANCE III 600 MHz spectrometer was been used to perform ligand based NMR spectroscopy as previously described [25, 26]. For CPMG NMR experiments, compounds were dissolved to a final concentration of 200 μM in the presence of 5% DMSO-d_6 and a gradient of 5,

10, 20 μ M CBP bromodomain proteins. For saturation transfer difference (STD) experiments, 10 μM CBP bromodomain protein was been used.

4.3.5 Crystallization

The crystal was grown at 4 °C using the sitting drop vapor diffusion technique. The crystal was grown using CBP bromodomain at approximately 1.5 mM concentration that was equilibrated with 20% (w/v) Polyethylene glycol 3,350, 0.2 M sodium phosphate monobasic monohydrate PH 4.7, and then a 1:1 mixture of paraffin oils and paratone was used to protect the crystal before it was frozen in liquid nitrogen. Structural data of DC-CPin7 in complex with CBP bromodomain have been deposited in the Protein Data Bank with the accession code 6LQX.

4.3.6 Microscale Thermophoresis

The binding affinity of DC-CPin711 was tested against CBP bromodomain protein using label-free microscale thermophoresis. The final concentration of the CBP bromodomain protein was kept constant at *ca.* 10 nM concentration, while the concentration of the compound DC-CPin711 was varied from 500 nM, and further diluted to 1:1 12 times in MST buffer (25 mM HEPES, pH 7.4, 150 mM NaCl, and 0.1% (*v/v*) pluronic). The samples were incubated for 5 min before they were loaded into label-free capillaries (Nanotemper Technologies). Data was collected at 25 °C in Monolith NT. Automated (Nanotemper Technologies). The excitation wavelength used was 280nm and the detection wavelength was 330nm. Data was analyzed using MO. Affinity Analysis software (Nanotemper Technologies) and GraphPad Prism. The K_d values were

determined in the MO. Affinity Analysis software (Nanotemper Technologies), using a K_d Fitting model.

4.3.7 Amplified Luminescent Proximity Homogeneous Assay

The amplified luminescent proximity homogeneous assays were performed as previously described[27]. The nickel chelate acceptor and streptavidin donor beads used in this assay were purchased from Perkin Elmer. The sequence of biotin-labelled H4 substrate peptide was SGRG-K(Ac)-GG-K(Ac)-GLG-K(Ac)-GGA-K(Ac)-RHRKVGG-K-Biotin (China Peptide, purity > 95%). The assay was performed in 20 μL of assay buffer containing 20 mM HEPES, pH 7.4, 0.1% bovine serum albumin (w/v), 1 mM DTT and 0.01% Triton X-100. All brodomains tested were incubated with compounds at room temperature for 15 min, biotin-labelled H4 peptide was added into OptiPlate-384 plate for 10 min. The final concentration of bromodomains and biotin-labelled H4 peptide were both 0.025 μM in this assay. Then the mixture of acceptor and donor beads were added and incubated for 60 min. The signals were then measured by EnVision microplate reader (PerkinElmer) and analyzed by GraphPad Prism 6.0.

4.3.8 Cell Lines

All cells were bought from the American Type Culture Collection (ATCC). All cells were maintained in the medium recommended by ATCC.org website at 37 °C with 5% CO_2.

4.3.9 Cell Proliferation Assays

All adherent cells were seeded in 96-well plates and allowed to adhere overnight. All suspension cells were transferred to 96-well plates and incubate for 1h before compound treatment. The cells were exposed with compounds for 96h. The fraction of viable cells was then

evaluated using CellTiter-Glo luminescent assays according to the manufacturer's instructions (Promega, G7572).

4.3.10 Western blot analysis

Cells were transferred to six-well plates and treated with DMSO or desired concentrations of compound for 48 h. The cells were fully lysed with SDS cell lysis buffer. SDS-polyacrylamide gel electrophoresis was performed to separate different proteins in the cell lysates and then the desired proteins were transferred to nitrocellulose membranes. The membranes were blocked using 5% skimmed milk in TBST for 30 minutes at room temperature and incubated with anti-c-Myc (Cell Signaling Technology, Cat # 5605S) and anti-GAPDH (Cell Signaling Technology, 5174S) primary antibody at 4 ° C overnight. Then, the blots were incubated with HRP-conjugated anti-rabbit IgG secondary antibody at room temperature for 1 h. After washing with TBST for 3 times, the bands were detected with an Amersham Imager 600 imaging system (GE Healthcare).

4.3.11 Cell Cycle and Apoptosis Assay

For the cell cycle assay, cells were transferred to 6-well plates and treated with or specified concentrations of DC-CPin711 or DMSO. Cells were collected and then washed 3 times with 800 μL of pre-cooled PBS after 48h of treatment. The cell pellet was resuspended by pre-cooled 70% (v/v) ethanol and fixed at 4 ° C overnight. The cells were washed again with PBS and then resuspended by propidium iodide / RNase solution (BD Pharmingen) for following cell cycle analysis. For the cell apoptosis analysis, cells were collected after 96h of exposure, and Annexin V-FITC Apoptosis Detection Kit (Keyen Biotech) was been used to detect cell apoptosis

according to the manufacturer's procedure. All samples were measured by FACSCalibur (BD Pharmingen), and data were analyzed by Modfit or FlowJo.

4.3.12 Statistical Analyses

Statistical analyses were conducted using GraphPad Prism 7.0. Unpaired two-tailed student's t test was used for the calculation of statistical significance. *$P<0.05$, **$P < 0.01$, ***$P < 0.001$, N.S. $P>0.05$.

Author contributions

Conception and design: B.Z and C.L.; Development of methodology: Y.C., X.B., F.Z. and Z.S. ; Acquisition of data: Y.C., X.B., F.Z., T.L., N.Z. and Z.S.; Analysis and interpretation of data: Y.C., X.B., F.Z., Z.S., P.X., W.L. ,H.J. and T.L. ;Writing, review, and/or revision of the manuscript: Y.C., X.B., F.Z., Z.S., H.J. ,W.L and C.L.; Administrative, technical, or material support: H.D., and N.Z.; Study supervision: H.J., K.C., H.D., B.Z., and C.L.

Declaration of competing interest

The authors declare no competing financial and non-financial interest.

Acknowledgements

References

[1] A.J. Bannister, T. Kouzarides, The CBP co-activator is a histone acetyltransferase, Nature

384(6610) (1996) 641-3.

[2] M. Delvecchio, J. Gaucher, C. Aguilar-Gurrieri, E. Ortega, D. Panne, Structure of the p300 catalytic core and implications for chromatin targeting and HAT regulation, Nat Struct Mol Biol 20(9) (2013) 1040-6.

[3] S. Mujtaba, Y. He, L. Zeng, S. Yan, O. Plotnikova, Sachchidanand, R. Sanchez, N.J. Zeleznik-Le, Z. Ronai, M.M. Zhou, Structural mechanism of the bromodomain of the coactivator CBP in p53 transcriptional activation, Mol Cell 13(2) (2004) 251-63.

[4] A.K. Jain, M.C. Barton, Bromodomain Histone Readers and Cancer, J Mol Biol 429(13) (2017) 2003-2010.

[5] F. Faiola, X. Liu, S. Lo, S. Pan, K. Zhang, E. Lymar, A. Farina, E. Martinez, Dual regulation of c-Myc by p300 via acetylation-dependent control of Myc protein turnover and coactivation of Myc-induced transcription, Mol Cell Biol 25(23) (2005) 10220-34.

[6] A.R. Conery, R.C. Centore, A. Neiss, P.J. Keller, S. Joshi, K.L. Spillane, P. Sandy, C. Hatton, E. Pardo, L. Zawadzke, A. Bommi-Reddy, K.E. Gascoigne, B.M. Bryant, J.A. Mertz, R.J. Sims, Bromodomain inhibition of the transcriptional coactivators CBP/EP300 as a therapeutic strategy to target the IRF4 network in multiple myeloma, Elife 5 (2016).

[7] K. Tsuboi, K. Hirayoshi, K. Takeuchi, H. Sabe, Y. Shimada, G. Ohshio, T. Tobe, M. Hatanaka, Expression of the c-myc gene in human gastrointestinal malignancies, Biochem Biophys Res Commun 146(2) (1987) 699-704.

[8] I. Bieche, I. Laurendeau, S. Tozlu, M. Olivi, D. Vidaud, R. Lidereau, M. Vidaud, Quantitation of MYC gene expression in sporadic breast tumors with a real-time reverse transcription-PCR assay, Cancer Res 59(12) (1999) 2759-2765.

[9] C.F. Rochlitz, R. Herrmann, E. deKant, Overexpression and amplification of c-myc during progression of human colorectal cancer, Oncology 53(6) (1996) 448-454.

[10] J.P. Dudley, J.A. Mertz, L. Rajan, M. Lozano, D.R. Broussard, What retroviruses teach us about the involvement of c-Myc in leukemias and lymphomas, Leukemia 16(6) (2002) 1086-1098.

[11] D.A. Hay, O. Fedorov, S. Martin, D.C. Singleton, C. Tallant, C. Wells, S. Picaud, M. Philpott, O.P. Monteiro, C.M. Rogers, S.J. Conway, T.P.C. Rooney, A. Tumber, C. Yapp, P. Filippakopoulos, M.E. Bunnage, S. Muller, S. Knapp, C.J. Schofield, P.E. Brennan, Discovery and Optimization of Small-Molecule Ligands for the CBP/p300 Bromodomains, J Am Chem Soc 136(26) (2014) 9308-9319.

[12] A.M. Taylor, A. Cote, M.C. Hewitt, R. Pastor, Y. Leblanc, C.G. Nasveschuk, F.A. Romero, T.D. Crawford, N. Cantone, H. Jayaram, J. Setser, J. Murray, M.H. Beresini, G.D. Boenig, Z.G. Chen, A.R. Conery, R.T. Cummings, L.A. Dakin, E.M. Flynn, O.W. Huang, S. Kaufman, P.J. Keller, J.R. Kiefer, T. Lai, Y.J. Li, J.P. Liao, W.F. Liu, H. Lu, E. Pardo, V. Tsui, J. Wang, Y.Y. Wang, Z.W. Xu, F. Yan, D. Yu, L. Zawadzke, X.Q. Zhu, X.Y. Zhu, R.J. Sims, A.G. Cochran, S. Bellon, J.E. Audia, S. Magnuson, B.K. Albrecht, Fragment-Based Discovery of a Selective and Cell-Active Benzodiazepinone CBP/EP300 Bromodomain Inhibitor (CPI-637), Acs Med Chem Lett 7(5) (2016) 531-536.

[13] T.D. Crawford, F.A. Romero, K.W. Lai, V. Tsui, A.M. Taylor, G.D. Boenig, C.L. Noland, J. Murray, J. Ly, E.F. Choo, T.L. Hunsaker, E.W. Chan, M. Merchant, S. Kharbanda, K.E. Gascoigne, S. Kaufman, M.H. Beresini, J.P. Liao, W.F. Liu, K.X. Chen, Z.G. Chen, A.R. Conery, A. Cote, H. Jayaram, Y. Jiang, J.R. Kiefer, T. Kleinheinz, Y.J. Li, J. Maher, E. Pardo,

F. Poy, K.L. Spillane, F. Wang, J. Wang, X.C. Wei, Z.W. Xu, Z.Y. Xu, I. Yen, L. Zawadzke, X.Y. Zhu, S. Bellon, R. Cummings, A.G. Cochran, B.K. Albrecht, S. Magnuson, Discovery of a Potent and Selective in Vivo Probe (GNE-272) for the Bromodomains of CBP/EP300, J Med Chem 59(23) (2016) 10549-10563.

[14] F.A. Romero, J. Murray, K.W. Lai, V. Tsui, B.K. Albrecht, L. An, M.H. Beresini, G.D. Boenig, S.M. Bronner, E.W. Chan, K.X. Chen, Z.G. Chen, E.F. Choo, K. Clagg, K. Clark, T.D. Crawford, P. Cyr, D.D. Nagata, K.E. Gascoigne, J.L. Grogan, G. Hatzivassiliou, W. Huang, T.L. Hunsaker, S. Kaufman, S.G. Koenig, R.N. Li, Y.J. Li, X.R. Liang, J.P. Liao, W.F. Liu, J. Ly, J. Maher, C. Masui, M. Merchant, Y.Q. Ran, A.M. Taylor, J. Wai, F. Wang, X.C. Wei, D. Yu, B.Y. Zhu, X.Y. Zhu, S. Magnuson, GNE-781, A Highly Advanced Potent and Selective Bromodomain Inhibitor of Cyclic Adenosine Monophosphate Response Element Binding Protein, Binding Protein (CBP), J Med Chem 60(22) (2017) 9162-9183.

[15] A.M.G. Thompson, O. Ursu, P. Babkin, C.V. Iancu, A. Whang, T.I. Oprea, J.Y. Choe, Discovery of a specific inhibitor of human GLUT5 by virtual screening and in vitro transport evaluation, Sci Rep-Uk 6 (2016).

[16] Y. Gao, J.B. Dickerson, F. Guo, J. Zheng, Y. Zheng, Rational design and characterization of a Rac GTPase-specific small molecule inhibitor, P Natl Acad Sci USA 101(20) (2004) 7618-7623.

[17] E.M. Bowers, G. Yan, C. Mukherjee, A. Orry, L. Wang, M.A. Holbert, N.T. Crump, C.A. Hazzalin, G. Liszczak, H. Yuan, C. Larocca, S.A. Saldanha, R. Abagyan, Y. Sun, D.J. Meyers, R. Marmorstein, L.C. Mahadevan, R.M. Alani, P.A. Cole, Virtual Ligand Screening of the p300/CBP Histone Acetyltransferase: Identification of a Selective Small Molecule Inhibitor,

Chemistry & Biology 17(5) (2010) 471-482.

[18] L.M. Lasko, C.G. Jakob, R.P. Edalji, W. Qiu, D. Montgomery, E.L. Digiammarino, T.M. Hansen, R.M. Risi, R. Frey, V. Manaves, B. Shaw, M. Algire, P. Hessler, L.T. Lam, T. Uziel, E. Faivre, D. Ferguson, F.G. Buchanan, R.L. Martin, M. Torrent, G.G. Chiang, K. Karukurichi, J.W. Langston, B.T. Weinert, C. Choudhary, P. de Vries, A.F. Kluge, M.A. Patane, J.H. Van Drie, C. Wang, D. McElligott, E. Kesicki, R. Marmorstein, C. Sun, P.A. Cole, S.H. Rosenberg, M.R. Michaelides, A. Lai, K.D. Bromberg, Discovery of a selective catalytic p300/CBP inhibitor that targets lineage-specific tumours, Nature 550(7674) (2017) 128-132.

[19] D. Spiliotopoulos, J. Zhu, E.C. Wamhoff, N. Deerain, J.R. Marchand, J. Aretz, C. Rademacher, A. Caflisch, Virtual screen to NMR (VS2NMR): Discovery of fragment hits for the CBP bromodomain, Bioorg Med Chem Lett 27(11) (2017) 2472-2478.

[20] P. Filippakopoulos, S. Picaud, O. Fedorov, M. Keller, M. Wrobel, O. Morgenstern, F. Bracher, S. Knapp, Benzodiazepines and benzotriazepines as protein interaction inhibitors targeting bromodomains of the BET family, Bioorgan Med Chem 20(6) (2012) 1878-1886.

[21] Q.Q. Wang, X.L. An, J.H. Xu, Y.W. Wang, L. Liu, E.L.H. Leung, X.J. Yao, Classical molecular dynamics and metadynamics simulations decipher the mechanism of CBP30 selectively inhibiting CBP/p300 bromodomains, Org Biomol Chem 16(35) (2018) 6521-6530.

[22] A. Hammitzsch, C. Tallant, O. Fedorov, A. O'Mahony, P.E. Brennan, D.A. Hay, F.O. Martinez, M.H. Al-Mossawi, J. de Wit, M. Vecellio, C. Wells, P. Wordsworth, S. Muller, S. Knapp, P. Bowness, CBP30, a selective CBP/p300 bromodomain inhibitor, suppresses human Th17 responses, P Natl Acad Sci USA 112(34) (2015) 10768-10773.

[23] L.J. Zou, Q.P. Xiang, X.Q. Xue, C. Zhang, C.C. Li, C. Wang, Q. Li, R. Wang, S. Wu, Y.L.

Zhou, Y. Zhang, Y. Xu, Y08197 is a novel and selective CBP/EP300 bromodomain inhibitor for the treatment of prostate cancer, Acta Pharmacol Sin 40(11) (2019) 1436-1447.

[24] J. Vervoorts, J.M. Luscher-Firzlaff, S. Rottmann, R. Lilischkis, G. Walsemann, K. Dohmann, M. Austen, B. Luscher, Stimulation of c-MYC transcriptional activity and acetylation by recruitment of the cofactor CBP, Embo Rep 4(5) (2003) 484-490.

[25] X. Kong, L. Chen, L. Jiao, X. Jiang, F. Lian, J. Lu, K. Zhu, D. Du, J. Liu, H. Ding, N. Zhang, J. Shen, M. Zheng, K. Chen, X. Liu, H. Jiang, C. Luo, Astemizole arrests the proliferation of cancer cells by disrupting the EZH2-EED interaction of polycomb repressive complex 2, J Med Chem 57(22) (2014) 9512-21.

[26] W.Y. Zhang, W.C. Lu, H. Jiang, Z.B. Lv, Y.Q. Xie, F.L. Lian, Z.J. Liang, Y.X. Jiang, D.J. Wang, C. Luo, J. Jin, F. Ye, Discovery of alkyl bis(oxy)dibenzimidamide derivatives as novel protein arginine methyltransferase 1 (PRMT1) inhibitors, Chem Biol Drug Des 90(6) (2017) 1260-1270.

[27] H. Jiang, J. Xing, C. Wang, H. Zhang, L.Y. Yue, X.Z. Wan, W. Chen, H. Ding, Y.Q. Xie, H.R. Tao, Z.F. Chen, H.L. Jiang, K.X. Chen, S.J. Chen, M.Y. Zheng, Y.Y. Zhang, C. Luo, Discovery of novel BET inhibitors by drug repurposing of nitroxoline and its analogues, Org Biomol Chem 15(44) (2017) 9352-9361.

Declaration of interests

☒   The authors declare that they have no known competing financial interests or personal relationships that could have appeared to influence the work reported in this paper.

☐The authors declare the following financial interests/personal relationships which may be considered as potential competing interests:
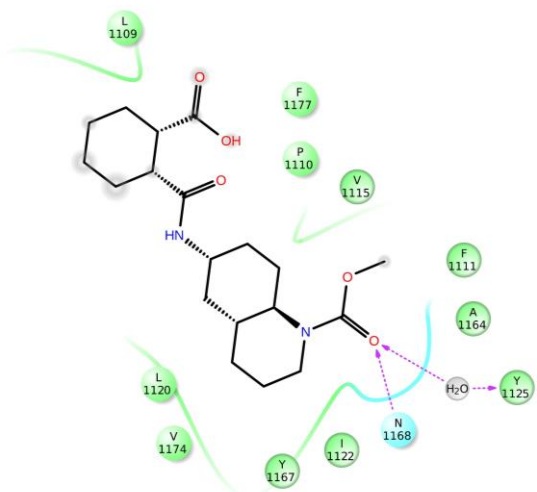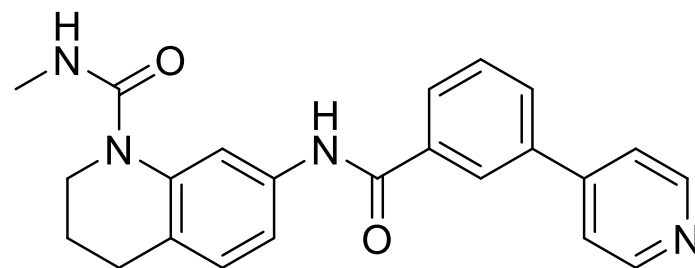
Crystal based iterative chemical optimization
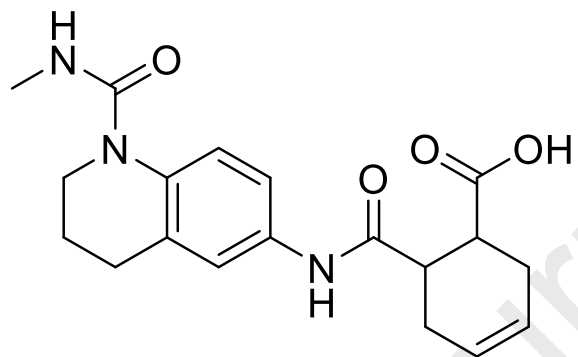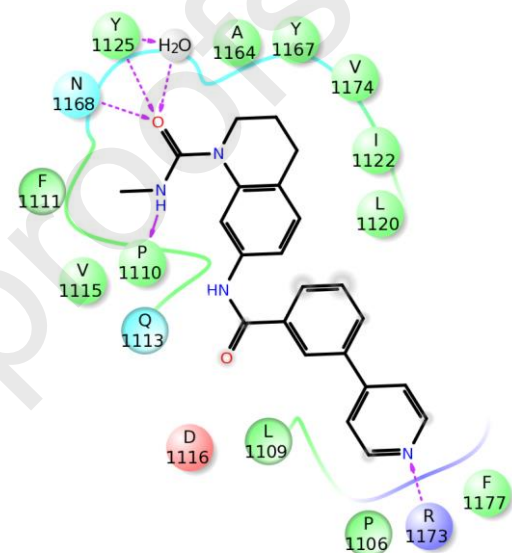
DC-CPin7
TR-FRET IC$_{50}$ = 2.5 μM

DC-CPin711
TR- FRET IC$_{50}$ = 63.3 nM

1. Two hit compounds of CBP bromodomain were discovered through virtual screening
2. A co-crystal of DC-CPin7 with CBP bromodomain was obtained
3. Crystal based chemical optimization were applied to improve potency
4. DC-CPin711 improved ~ 40-fold potency by chemical optimization
5. DC-CPin711 showed decent anti leukemia effects